

# Normal boundary intersection method based on principal components and Taguchi's signal-to-noise ratio applied to the multiobjective optimization of 12L14 free machining steel turning process

D. M. D. Costa<sup>1</sup> · T. I. Paula<sup>1</sup> · P. A. P. Silva<sup>1</sup> · A. P. Paiva<sup>1</sup>

Received: 15 October 2015 / Accepted: 1 February 2016 / Published online: 1 March 2016  
© Springer-Verlag London 2016

**Abstract** When it comes to multiobjective optimization problems, the challenge is to find a solution that satisfies all the answers simultaneously. When the responses are correlated and present conflicting objectives, it is even more difficult to find an adequate solution, since most optimization techniques do not consider this information. The objective of this work is to apply Taguchi's signal-to-noise ratio (SNR) and principal component analysis (PCA) in order to standardize the optimization objectives, eliminate the correlation between the multiple responses, and combine them with the normal boundary intersection (NBI) method to perform a proper optimization. A case study of 12L14 free machining steel turning process is used, since it is considered an important machining operation. Three input parameters (cutting speed, feed rate, and depth of cut) and three response variables (mean roughness, total mean roughness, and removal rate) were considered. Response surface methodology was employed to build the objective functions. The NBI-PCA-SNR method was successfully applied, presenting viable solutions.

**Keywords** Multiobjective optimization · Normal boundary intersection · Taguchi's signal-to-noise ratio · Principal component analysis

## 1 Introduction

When dealing with multiobjective optimization problems (MOP), under various circumstances, the multiple responses considered in a process may present conflicting objectives, with individual optimization leading to different solution sets [1]. Thus, the task is to find a vector of decision variables that satisfies, at the same time, the objective functions and the constraints and also provides an acceptable value for each response [2, 3]. Fortunately, many techniques can be applied to solve multiobjective optimization problems. Among those techniques is the normal boundary intersection (NBI) method. The NBI method, proposed by Das and Dennis [4], is a method for generating Pareto surface for linear and also for nonlinear multiobjective optimization problems. It is proved that this method is independent of the relative scales of the objective functions and that it is successful in producing an evenly distributed set of points in the Pareto surface given an evenly distributed set of parameters [4–6], which is its advantage over conventional methods.

Although this method can be very useful for the optimization of countless processes, it may conduct the results to inadequate optimum points if the responses are correlated and present conflicting objectives. This drawback may be reversed if the Pareto frontier is designed with uncorrelated functions represented by the scores obtained by the principal component analysis (PCA) [7]. PCA extracts the eigenvectors from the variance-covariance or the correlation matrix using them as weights that are used to multiply the standardized values of original data set [8–15]. Still, if there are variables in the set

---

✉ A. P. Paiva  
andersonppaiva@unifei.edu.br

D. M. D. Costa  
danielle.costa@ifsuldeminas.edu.br

T. I. Paula  
taynaraincerti@unifei.edu.br

P. A. P. Silva  
paty\_agnes@yahoo.com.br

<sup>1</sup> Institute of Industrial Engineering and Management, Federal University of Itajuba, Itajuba, Minas Gerais, Brazil

with inverse directions of optimization, the maximization or minimization of the principal components will favor some variables and not others. An alternative for this drawback is to apply the Taguchi's signal-to-noise ratio (SNR) before principal components analysis [16]. Once modeled, this new data set may be optimized by the NBI method, which often leads to a continuous Pareto frontier.

The objective of this work is to apply PCA and SNR in order to eliminate the correlation between the multiple responses and different optimization objectives and then combine them with the NBI method. This approach proposed is called the NBI-PCA-SNR method. A step-by-step procedure was developed for this purpose. To demonstrate its applicability, a case study of 12L14 free machining steel turning process is used.

The free machining steel turning process is characterized as an important operation in the modern industry, since the free machining steels are developed to offer good machining conditions and excellent chip, appliances, and components to pumps, plugs, and connections [1, 10]. An important characteristic of this process is the presence of correlation between its responses, which have different optimization objectives. For example, while the roughness has to be minimized, the removal rate has to be maximized. In this work, the optimized responses included the mean roughness, total roughness, and material removal rate. As input parameters, the cutting speed, feed rate, and depth of cut were considered.

This paper is organized as follows: Section 2 presents the concepts of multiobjective optimization problems and the main characteristics of the normal boundary Intersection method and also the concepts of principal component analysis and signal-to-noise ratio, discussing their applications; Section 3 presents the NBI-PCA-SNR method that is proposed in this study; Section 4 presents a numerical application to illustrate the adequacy of the study's proposal, while Section 5 presents this study's conclusions.

## 2 Multiobjective optimization techniques for correlated functions

In order to overcome the disadvantages of the traditional multiobjective optimization techniques, Das and Dennis [4] proposed the normal boundary intersection method, showing that this technique is independent of the relative scales of the functions and it is successful in producing an evenly distributed set of points in the Pareto set.

The first step in the NBI method establishes the payoff matrix ( $\Phi$ ), based on the calculation of the individual minima of each objective function. The optimal solution for the  $i$ th objective function  $f_i(x)$  can be represented as  $f_i^*(x_i^*)$ . When the individual optimum  $x_i^*$  is replaced in the remaining

objective functions  $f_i^*(x_i^*)$  is obtained. In matrix notation, the payoff matrix can be written as [6]:

$$\Phi = \begin{bmatrix} f_1^*(x_1^*) & \cdots & f_1(x_i^*) & \cdots & f_1(x_m^*) \\ \vdots & \ddots & \vdots & \ddots & \vdots \\ f_i(x_1^*) & \cdots & f_i^*(x_i^*) & \cdots & f_i(x_m^*) \\ \vdots & \ddots & \vdots & \ddots & \vdots \\ f_m(x_1^*) & \cdots & f_m(x_i^*) & \cdots & f_m^*(x_m^*) \end{bmatrix} \quad (1)$$

The set of individual optimal solutions,  $f^U = [f_1^*(x_1^*), \dots, f_i^*(x_i^*), \dots, f_m^*(x_m^*)]^T$ , is known as the Utopia point, while the set of the solutions that are most distant from the optimal solutions,  $f^N = [f_1^N, \dots, f_i^N, \dots, f_m^N]^T$ , is known as the Nadir point [4]. Thus, the payoff matrix can be normalized using Eq. (2):

$$\bar{f}(x) = \frac{f_i(x) - f_i^U}{f_i^N - f_i^U}, \quad i = 1, \dots, m \quad (2)$$

This normalization  $\text{Min } \bar{f}_1(\mathbf{x}) \text{ s.t. : } \bar{f}_1(\mathbf{x}) - \bar{f}_2(\mathbf{x}) + 2w - 1 = 0, g_j(\mathbf{x}) \geq 0, 0 \leq w \leq 1$  leads to the normalized payoff matrix ( $\bar{\Phi}$ ) and the vector  $\bar{\mathbf{F}}(\mathbf{x})$ . Associated to vector of weights ( $\beta$ ) and a unitary normal vector ( $\hat{\mathbf{n}}$ ), the classical NBI formulation can be described as [6]:

$$\begin{aligned} & \text{Max } D \\ & \text{(x,t)} \\ & \text{s.t. : } \bar{\Phi}\beta + D\hat{\mathbf{n}} = \bar{\mathbf{F}}(\mathbf{x}) \\ & \quad \mathbf{x} \in \Omega \\ & \quad g_j(\mathbf{x}) \leq 0 \\ & \quad h_j(\mathbf{x}) \leq 0 \end{aligned} \quad (3)$$

The conceptual parameter  $D$  can be algebraically eliminated from Eq. (3), such that, for bi-dimensional problem, this expression can be written as [6]:

$$\begin{aligned} & \text{Min } \bar{f}_1(\mathbf{x}) \\ & \text{s.t. : } \bar{f}_1(\mathbf{x}) - \bar{f}_2(\mathbf{x}) + 2w - 1 = 0 \\ & \quad g_j(\mathbf{x}) \geq 0 \\ & \quad 0 \leq w \leq 1 \end{aligned} \quad (4)$$

where  $\bar{f}_1(\mathbf{x})$  and  $\bar{f}_2(\mathbf{x})$  are the normalized objective functions,  $g_j(\mathbf{x}) \geq 0$  and  $0 \leq w \leq 1$  are the set of constraints for experimental region and the cuboidal region, respectively.

This optimization problem can be iteratively solved for different values of  $w$ , creating an evenly distributed Pareto frontier. A common choice for  $w$  is suggested by Jia and Ierapetritou [5] as  $w_n = 1 - \sum_{i=1}^n w_i$ .

The NBI method previously described is widely employed to generate the trade-off solutions for nonlinear multiobjective optimization problems. However, if the several objective functions are positively correlated and present conflicting objectives among themselves, the NBI method tends to fail and to produce unreal results and non-convex frontiers. In addition, the correlation among the responses can substantially

influence the values of the  $y(x, z)$  regression coefficients and it cannot be neglected [7]. The individual analysis of each response may lead to a conflicting optimum [7, 11, 16]. One may deal with this impeding correlation influence by employing principal components analysis.

According to Paiva et al. [11], PCA is a recognized dimensionality reduction technique, which has the characteristic of preserving most of the information contained in the original set of variables. According to Zhang et al. [17], based on the variance-covariance matrix, the PCA method proceeds in such a way that the first principal component has the highest variance, and each succeeding component in turn has the highest possible variance within the constraint.

Supposing that some objective functions  $f_1(x), f_2(x), \dots, f_p(x)$  are correlated with values written in terms of a random vector  $Y^T = [Y_1, Y_2, \dots, Y_p]$  and assuming that  $\Sigma$  is the variance-covariance matrix associated to this vector, then  $\Sigma$  can be factorized in pairs of eigenvalues-eigenvectors  $(\lambda_i, e_i), \dots \geq (\lambda_p, e_p)$ , where  $(\lambda_1 \geq \lambda_2 \geq \dots \geq \lambda_p \geq 0)$ , such as the  $i$ th uncorrelated linear combination may be stated as  $PC_1 = e_i^T Y = e_{1i} Y_1 + e_{2i} Y_2 + \dots + e_{pi} Y_p$ , with  $i = 1, 2, \dots, p$ .

The  $i$ th principal component can be obtained as maximization of this linear combination. A set of original variables can be replaced by uncorrelated linear combinations of the form scores of the principal component that can be expressed in terms of a score matrix, defined as [18]:

$$PC_k = Z^T E$$

$$= \begin{bmatrix} \left( \frac{x_{11} - \bar{x}_1}{\sqrt{s_{11}}} \right) & \left( \frac{x_{21} - \bar{x}_2}{\sqrt{s_{22}}} \right) & \dots & \left( \frac{x_{p1} - \bar{x}_p}{\sqrt{s_{pp}}} \right) \\ \left( \frac{x_{12} - \bar{x}_1}{\sqrt{s_{11}}} \right) & \left( \frac{x_{22} - \bar{x}_2}{\sqrt{s_{22}}} \right) & \dots & \left( \frac{x_{p2} - \bar{x}_p}{\sqrt{s_{pp}}} \right) \\ \vdots & \vdots & \ddots & \vdots \\ \left( \frac{x_{1n} - \bar{x}_1}{\sqrt{s_{11}}} \right) & \left( \frac{x_{2n} - \bar{x}_2}{\sqrt{s_{22}}} \right) & \dots & \left( \frac{x_{pn} - \bar{x}_p}{\sqrt{s_{pp}}} \right) \end{bmatrix}^T \times \begin{bmatrix} e_{11} & e_{12} & \dots & e_{1p} \\ e_{21} & e_{22} & \dots & e_{2p} \\ \vdots & \vdots & \ddots & \vdots \\ e_{p1} & e_{p2} & \dots & e_{pp} \end{bmatrix} \tag{5}$$

Being  $x_{pn}$  a random observation,  $x_p$  the  $p$ th average response,  $\sqrt{s_{pp}}$  the standard deviation,  $p$  the response, and  $[E]$  the eigenvectors of the multivariate set.

However, if there are variables in the set with optimization in verse direction, i.e., responses that need to be minimized while others need to be maximized, the maximization or minimization of the principal components will favor some variables and harm others.

To analyze the maximization or minimization influence of the principal components on the variables, it is necessary to observe the correlation between them. For example, if the first principal component ( $PC_1$ ) maintains a negative correlation with certain variables and we desire to minimize them, then  $PC_1$  maximization leads to their minimization. Thus, if the correlation between  $PC_1$  and a group of variables is positive, its

maximization or minimization will imply the maximization or minimization of each original response variable. If the correlation is negative, the optimization senses will be inverse [11].

In case there is a positive correlation with some variables and negative correlation with other simultaneously, multiplying the original response by a negative constant will solve the problem. This multiplication should be done before proceeding to the analysis of the principal component. However, when the responses have different optimization objective, another likely alternative is to apply the Taguchi’s signal-to-noise ratio.

Taguchi uses the SNR to measure the quality characteristic deviating from the desired value and these characteristics vary depending on the type of problem under study, which may be classified as “smaller-the-better” and “bigger-the-better” [19–21]. Their mathematical expressions are represented by the Eqs. (6) and (7), respectively, where  $y$  denotes the performance indicator, subscript  $i$  is the experiment number and  $N$  is the number of replicates of the experiment  $i$ . After the transformation, SNR must always be maximized, which makes it possible to standardize the optimization objectives for the individual responses.

$$SNR = -10 \log_{10} \left( \frac{\sum_{i=1}^N y_i^2}{N} \right) \tag{6}$$

$$SNR = -10 \log_{10} \left( \frac{\sum_{i=1}^N 1/y_i^2}{N} \right) \tag{7}$$

### 3 The NBI-PCA-SNR method

Given the aforementioned discussion, this work proposes a combination of techniques which, applied together, may conduct to acceptable solutions for correlated multiobjective problems with conflicting objectives. Then, a hybrid method based on principal component analysis, Taguchi’s signal-to-noise ratio, and the normal boundary intersection, called NBI-PCA-SNR method, is proposed. For a better understanding of this proposal, a step-by-step procedure was developed, as it follows:

Step 1: Experimental design and analysis

The different responses can be modeled by using the design of experiments. An experimental matrix is set, the experiments are run in random order, and the responses are stored. Then, applying the *OLS* algorithm, it is possible to define the models for the responses.

Step 2: Individual constrained optimization

The response targets, that in this study are the individual optimums  $(\zeta_{vj})$ , are established using the

individual constrained optimization of each response, where  $\zeta_{y_i} = \text{Min}_{\mathbf{x} \in \Omega} [\hat{y}_j(\mathbf{x})]$  or  $\zeta_{y_i} = \text{Max}_{\mathbf{x} \in \Omega} [\hat{y}_j(\mathbf{x})]$ , depending on the response optimization objective.

Step 3: Correlation analysis

The correlation analysis allows the identification of the presence of correlation between the responses.

Step 4: Taguchi’s signal-to-noise ratio

The Taguchi’s signal-to-noise ratio is applied for the original responses by using Eqs. (6) and (7), according to the optimization objective of each response. After the application of SNR, all the responses must be maximized, crossing off the problem caused by the conflicting objectives of the original responses.

Step 5: Principal component analysis

Principal components analysis is applied for the set of pre-processed responses. Using the correlation matrix, PC scores must be extracted and stored with the respective eigenvalues and eigenvectors. Then, it is selected the number of PCs required to explain at least 90 % of variance model. With the application of PCA, the correlation between the responses is eliminated, and it is possible to proceed with the optimization by the NBI method.

Step 6: Response modeling

The OLS algorithm is applied for the PCs, the results are analyzed and the equations for the principal components are established. These models are the new responses of the optimization problem.

Step 7: Payoff matrix and scalarization

The first step to determinate the payoff matrix for the NBI method is the individual constrained maximization of the PCs modeled in step 6. With the individual optimization of the PCs, the Utopia ( $f^U = PC^{\max}$ ) and the Nadir ( $f^N = PC^{\min}$ )

points can be found and the Payoff Matrix ( $\Phi$ ) for a bivariate case can be written as:

$$\Phi = \begin{bmatrix} PC_1^{\max}(\mathbf{x}) & PC_1^{\min}(\mathbf{x}) \\ PC_2^{\min}(\mathbf{x}) & PC_2^{\max}(\mathbf{x}) \end{bmatrix} \tag{8}$$

With these payoff matrix values, the scalarization of PC<sub>1</sub> and PC<sub>2</sub> can be promoted. For a bivariate case, it is given by Eq. (9):

$$\bar{f}(x) = \frac{f_i(x) - f_i^U}{f_i^N - f_i^U} \tag{9}$$

$$\Rightarrow \begin{cases} \bar{f}_1(x) = \overline{PC}_1(\mathbf{x}) = \frac{PC_1(\mathbf{x}) - PC_1^{\max}}{PC_1^{\min} - PC_1^{\max}} \\ \bar{f}_2(x) = \overline{PC}_2(\mathbf{x}) = \frac{PC_2(\mathbf{x}) - PC_2^{\max}}{PC_2^{\min} - PC_2^{\max}} \end{cases}$$

Step 8: NBI method and the Pareto frontier

The optimization by the NBI method is applied according to Eq. (10), which must be solved for different values of  $w$ , leading to the construction of the Pareto frontier.

$$\text{Min} \left( \frac{PC_i(\mathbf{x}) - PC_i^l(\mathbf{x})}{PC_i^{\max}(\mathbf{x}) - PC_i^l(\mathbf{x})} \right)$$

$$s.t. : \left( \frac{PC_1(\mathbf{x}) - PC_1^l(\mathbf{x})}{PC_1^{\max}(\mathbf{x}) - PC_1^l(\mathbf{x})} \right) - \left( \frac{PC_2(\mathbf{x}) - PC_2^l(\mathbf{x})}{PC_2^{\max}(\mathbf{x}) - PC_2^l(\mathbf{x})} \right) + 2w - 1 = 0$$

$$\mathbf{x}^T \mathbf{x} \leq \rho$$

$$0 \leq w \leq 1 \tag{10}$$

**Fig. 1** Distribution of measurement points in each workpiece (a). Rugosimeter used in measurements of output variables (b)

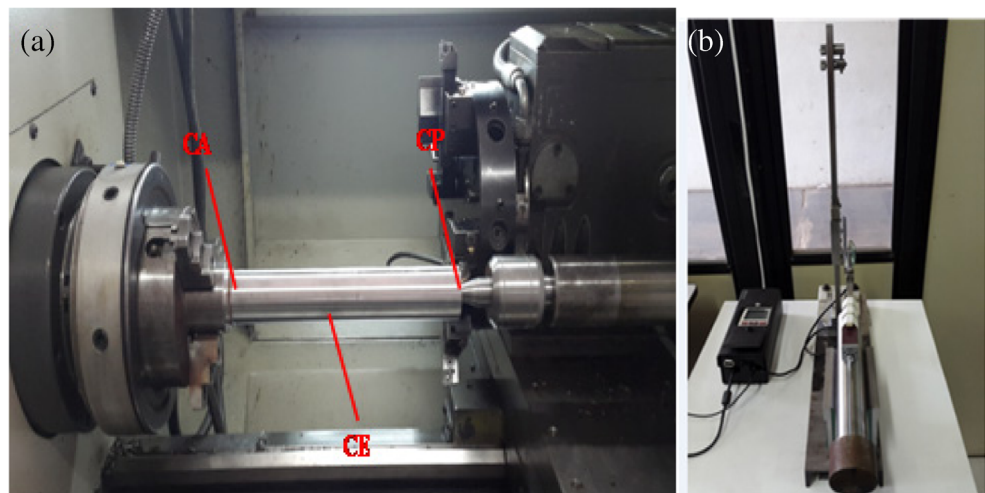


**Table 1** Control factors and respective levels [1]

Parameters	Symbol	Unit	Levels (uncoded and coded)				
			-1.682	-1	0	+1	+1.682
Cutting speed	<i>V</i>	m/min	180	220	280	340	380
Feed rate	<i>f</i>	mm/rev	0.07	0.08	0.10	0.12	0.13
Depth of cut	<i>d</i>	mm	0.53	0.70	0.95	1.20	1.37

## 4 Optimization of the 12L14 free machining steel turning

### 4.1 Workpiece material

In this investigation, 12L14 free machining steel (0.09 % C; 0.03 % Si; 1.24 % Mn; 0.046 % P; 0.273 % S; 0.15 % Cr; 0.08 % Ni; 0.26 % Cu; 0.001 % Al; 0.02 % Mo; 0.28 % Pb; 0.0079 % N<sub>2</sub>), with dimensions of φ40 × 295 mm was selected as the workpiece material for the turning process.

### 4.2 Experimental setup

The turning experiments were conducted on a NARDINI CNC lathe, with 7.5 cv power and maximum rotation of 4000 rpm. The hard metal inserts (ISO P35 code SNMG 090304 – PM, Sandvik class GC 4035) were coated with three

layers (Ti(C,N), Al<sub>2</sub>O<sub>3</sub>, TiN) and a tool holder ISO code DSBNL 1616H09.

The metrics of surface roughness were measured in three points of the workpiece: chestnut (CA), center (CE), and counterpoint (CP) (Fig. 1a) and then, all roughness responses were assessed using a Mitutoyo portable roughness meter, model Surftest SJ 201 (Fig. 1b). Note that value roughness in the CA point tends to be smaller than the value roughness in the CP point, since, in the CA point, the workpiece is fixed and in the CP point, it is not fixed. Material removal response rates were calculated.

### 4.3 Application of the NBI-PCA-SNR method

Step 1: Experimental design and analysis

Given that the objective functions were initially unknown, they were modeled using the response surface methodology (RSM). A sequential set of 17 experimental runs was established using a central composite design (CCD) with three parameters  $2^k = 2^3 = 8$  at two levels, six axial points  $2k = 6$  and three center points. The adopted value for axial distance  $\alpha$  was 1.682. The experimental planning was performed at three different levels of cutting parameters: cutting speed (*V*), feed rate (*f*), and depth of cut (*d*), as shown in Table 1. Three different outputs were measured: mean roughness ( $R_a$ ), total mean

**Table 2** Experimental data for the 12 L14 free machining steel turning

Parameters			Responses			Responses (SNR)			Responses (PCA)	
<i>V</i> [m/min]	<i>f</i> [mm/rev]	<i>d</i> [mm]	$R_a$	$R_t$	MRR	SNR/ $R_a$	SNR/ $R_t$	SNR/MRR	PC <sub>1</sub>	PC <sub>2</sub>
220	0.08	0.70	1.36	9.53	12.32	-2.69	-19.59	21.81	3.35	-0.23
340	0.08	0.70	1.65	11.24	19.04	-4.36	-21.01	25.59	1.29	-0.15
220	0.12	0.70	1.78	10.08	18.48	-5.02	-20.07	25.33	1.47	0.06
340	0.12	0.70	1.84	10.39	28.56	-5.29	-20.34	29.12	0.59	0.87
220	0.08	1.20	2.22	14.73	21.12	-6.91	-23.37	26.49	-1.12	-1.32
340	0.08	1.20	2.21	13.82	32.64	-6.89	-22.81	30.28	-1.48	-0.13
220	0.12	1.20	1.82	11.29	31.68	-5.21	-21.06	30.02	0.15	0.81
340	0.12	1.20	2.24	13.35	48.96	-6.99	-22.51	33.80	-1.96	0.87
180	0.10	0.95	1.90	13.01	17.10	-5.56	-22.28	24.66	0.31	-1.11
380	0.10	0.95	2.09	13.40	36.10	-6.39	-22.54	31.15	-1.27	0.29
280	0.07	0.95	1.85	10.84	18.62	-5.35	-20.70	25.40	1.02	-0.24
280	0.13	0.95	1.85	10.85	34.58	-5.33	-20.71	30.78	0.13	1.13
280	0.10	0.53	1.68	8.95	14.84	-4.51	-19.03	23.43	2.50	0.09
280	0.10	1.37	2.31	13.77	38.36	-7.26	-22.78	31.68	-1.86	0.18
280	0.10	0.95	2.32	12.57	26.60	-7.31	-21.98	28.50	-0.99	-0.31
280	0.10	0.95	2.24	12.73	26.60	-7.00	-22.10	28.50	-0.90	-0.31
280	0.10	0.95	2.38	13.00	26.60	-7.54	-22.28	28.50	-1.23	-0.47

**Table 3** Estimated coefficients and predictive statistics of the response

Coefficient	$R_a$	$R_t$	MRR	SNR/ $R_a$	SNR/ $R_t$	SNR/MRR	PC <sub>1</sub>	PC <sub>2</sub>
Constant	2.316	12.761	26.600	-7.298	-22.117	28.498	-1.046	-0.367
$V$	0.079	0.280	5.679	-0.373	-0.222	1.907	-0.590	0.329
$f$	0.017	-0.307	5.082	-0.119	0.204	1.694	-0.241	0.494
$d$	0.212	1.469	6.997	-0.971	-1.101	2.387	-1.350	-0.014
$V*V$	-0.121	0.168	0.000	0.510	-0.114	-0.211	0.216	-0.013
$f*f$	-0.172	-0.664	0.000	0.736	0.489	-0.146	0.588	0.290
$d*d$	-0.121	-0.484	0.000	0.544	0.418	-0.335	0.498	0.180
$V*f$	0.023	0.198	1.140	-0.049	-0.106	0.000	-0.072	-0.052
$V*d$	0.008	-0.109	1.500	0.024	0.100	0.000	0.057	0.045
$f*d$	-0.122	-0.451	1.400	0.608	0.302	0.000	0.419	0.228
Adj. $R^2$ (%)	86.20	81.64	99.72	82.94	82.75	99.82	92.11	80.41
Regression ( $p$ value)	0.030	0.007	- <sup>a</sup>	0.003	0.004	0.000	0.000	0.005
Lack of Fit ( $p$ value)	0.290	0.062	- <sup>a</sup>	0.165	0.055	- <sup>a</sup>	0.107	0.071
Normality (AD) test	0.513	0.108	1.179	0.350	0.131	0.287	0.180	0.248
AD ( $p$ value)	0.166	0.992	<0.005	0.430	0.977	0.576	0.900	0.710
Curvature ( $p$ value)	0.013	0.023	- <sup>a</sup>	0.010	0.016	- <sup>a</sup>	0.008	0.018

The italicized values represent the individually significant terms at 95 % CI

<sup>a</sup> The test does not apply to the response

roughness ( $R_t$ ), and removal rate ( $MRR$ ). The experimental matrix is presented in Table 2.

The OLS algorithm was applied, and the ANOVA procedure was used to check the adequacy of the models as well as their adjustment. Table 3 presents the coefficients for the final full quadratic models and the main results of the ANOVA.

All regression  $p$  values were lower than the significance of 5 %, and no lack of fit was observed. The models presented adj- $R_2$  values above 80.0 % indicating their adequacy. The normality test for the residuals of the RSM models indicated that the residuals are normal. Therefore, the ANOVA results show that the final full quadratic models are reliable and can be used for the optimization of this end milling process. Figure 2 presents the response surface graphics for the most significant turning parameters on which the analysis can be done.

**Step 2: Individual constraint optimization**

Target values for the responses modeled in step 1 were established using the individual constrained minimization for  $R_a$  and  $R_t$ , such as Eqs. (11) and (12), and the individual constrained maximization of response MRR, such as Eq. (13) where  $\mathbf{x}=[V,f,d]$ .

$$\zeta_{R_a} = \text{Min}_{\mathbf{x} \in \Omega} [\hat{R}_{a_i}(\mathbf{x})] \tag{11}$$

$$\zeta_{R_t} = \text{Min}_{\mathbf{x} \in \Omega} [\hat{R}_{t_i}(\mathbf{x})] \tag{12}$$

$$\zeta_{MRR} = \text{Max}_{\mathbf{x} \in \Omega} [\hat{MRR}_i(\mathbf{x})] \tag{13}$$

The target values established by the individual optimizations were as follows:  $\zeta_{R_a} = 1.45$ ,  $\zeta_{R_t} = 8.75$ , and  $\zeta_{MRR} = 47.78$ .

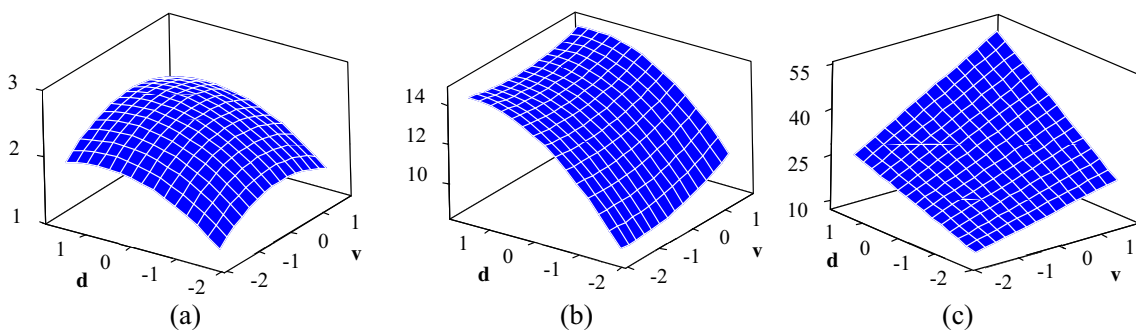


**Fig. 2** Response surfaces for  $R_a$  (a),  $R_t$  (b), and MRR (c). Hold value:  $f=0$

**Table 4** Correlation structure between the responses

	$R_a$	$R_t$	MRR	PC <sub>1</sub>
$R_t$	0.834 (0.000)			
MRR	0.596 (0.012)	0.591 (0.033)		
PC <sub>1</sub>	-0.937 (0.000)	-0.896 (0.000)	-0.779 (0.000)	
PC <sub>2</sub>	-0.174 (0.505)	-0.369 (0.145)	0.587 (0.013)	-0.000 (1.000)

Cell contents: Pearson correlation (P value)

**Step 3: Correlation analysis**

Using correlation analysis (Table 4), the existence of a strong correlation, with statistical significance, between the responses  $R_a$  and  $R_t$ , a moderate correlation between  $R_a$  and MRR, and also a moderate correlation between  $R_t$  and MRR can be observed.

**Step 4: Taguchi’s signal-to-noise ratio**

The Taguchi’s signal-to-noise ratio was calculated according to Eq. (6) for  $R_a$  and  $R_t$  and according to Eq. (7) for MRR. The calculated values for  $NR/R_a$ ,  $NR/R_t$ , and  $NR/MRR$  are presented in Table 2. The OLS algorithm was applied for  $SNR/R_a$ ,  $SNR/R_t$ , and  $SNR/MRR$ , and the results can be observed in Table 3. The ANOVA results show that the final full quadratic models are reliable and can be used for the optimization of this process.

**Step 5: Principal component analysis**

Using the correlation matrix, principal components scores were extracted with their respective eigenvalues and eigenvectors, as shown in Table 5. It was observed that the two principal components explain 94.9 % of the variance-covariance structure established between the surface responses, with eigenvalues greater than one unit. Therefore, the optimization will proceed using the scores of the two first principal components. The scores of the transformed data for PC<sub>1</sub> and PC<sub>2</sub> are presented in Table 3.

**Step 6: Response modeling**

As it has been mentioned, the PCA obtains

**Table 5** Principal component analysis:  $SNR/R_a$ ,  $SNR/R_t$ , and  $SNR/MRR$

	PC <sub>1</sub>	PC <sub>2</sub>	PC <sub>3</sub>
Eigenvalue ( $e$ )	2.4023	0.4451	0.1526
Proportion	0.801	0.148	0.051
Cumulative	0.801	0.949	1.000
Eigenvectors ( $\delta$ )			
NR/ $R_a$	0.608	0.226	-0.761
NR/ $R_t$	0.584	0.521	0.622
NR/MRR	-0.537	0.823	-0.185

**Table 6** Optimization results for NBI-PCA-SNR approach

(w)	Responses		Uncoded parameters			Uncoded responses			GPE
	PC <sub>1</sub> (x)	PC <sub>2</sub> (x)	V	f	d	$R_a$	$R_t$	MMR	
0.00	-0.40	1.43	296.41	0.13	1.09	1.92	11.11	42.08	0.716
0.05	-0.11	1.40	286.18	0.13	1.04	1.88	10.75	39.23	0.705
0.10	0.09	1.34	278.94	0.13	1.00	1.86	10.51	36.80	0.714
0.15	0.26	1.26	273.50	0.13	0.96	1.85	10.33	34.61	0.730
0.20	0.41	1.18	269.39	0.13	0.92	1.84	10.20	32.59	0.752
0.25	0.55	1.09	266.32	0.13	0.88	1.84	10.09	30.70	0.776
0.30	0.67	0.99	264.20	0.13	0.84	1.83	9.99	28.93	0.801
0.35	0.80	0.90	262.97	0.13	0.80	1.83	9.90	27.26	0.825
0.40	0.93	0.80	262.63	0.13	0.77	1.83	9.82	25.67	0.849
0.45	1.06	0.71	263.16	0.13	0.73	1.83	9.74	24.17	0.871
0.50	1.20	0.62	264.63	0.13	0.69	1.83	9.66	22.74	0.889
0.55	1.34	0.53	267.08	0.12	0.66	1.82	9.57	21.39	0.904
0.60	1.51	0.45	270.68	0.12	0.62	1.81	9.49	20.12	0.913
0.65	1.69	0.37	275.58	0.12	0.59	1.79	9.40	18.92	0.915
0.70	1.89	0.31	282.32	0.11	0.56	1.76	9.32	17.80	0.907
0.75	2.12	0.26	291.70	0.11	0.54	1.71	9.24	16.81	0.883
0.80	2.39	0.22	303.69	0.10	0.54	1.62	9.20	15.99	0.834
0.85	2.70	0.20	301.85	0.09	0.56	1.54	9.06	15.16	0.778
0.90	2.96	0.16	290.06	0.09	0.57	1.49	8.88	14.33	0.744
0.95	3.14	0.09	275.52	0.08	0.58	1.47	8.79	13.66	0.733
1.00	3.22	-0.03	259.02	0.08	0.59	1.47	8.88	13.18	0.749

The italicized values are the optimal by the minimization of the global percent error (GPE)

uncorrelated objective functions (-0.000,  $p$  value=1.000, Table 4). Applying the OLS algorithm for PC<sub>1</sub> and PC<sub>2</sub>, the following equations were obtained:

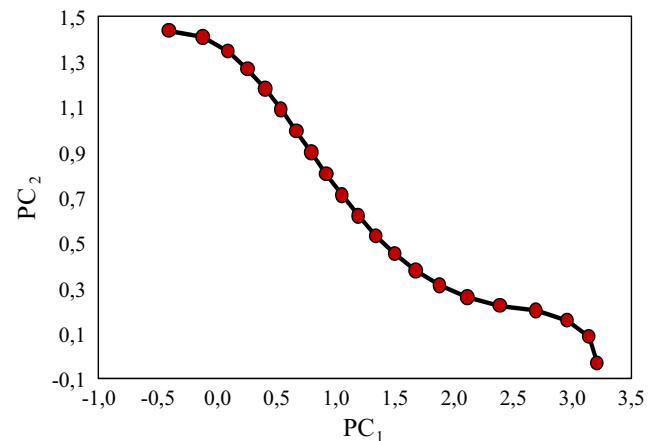


**Fig. 3** Pareto frontier obtained for the NBI-PCA-SNR approach

**Table 7** Convexity of the objective functions

	PC <sub>1</sub>	PC <sub>2</sub>
Eigenvalues	0.757	0.362
	0.345	0.117
	0.200	-0.022
	Convex	Saddle

$$PC_1 = -1.046 - 0.590V - 0.241f - 1.350d + 0.216V^2 + 0.588f^2 + 0.498d^2 - 0.072Vf + 0.057Vd + 0.419fd \tag{14}$$

$$PC_2 = -0.367 + 0.329V + 0.494f - 0.014d - 0.013V^2 + 0.290f^2 + 0.180d^2 - 0.052Vf + 0.045Vd + 0.228fd \tag{15}$$

This analysis was considered for a level of significance of 5 %, and all the models presented adj. *R*<sup>2</sup> values above 80.0 % and no lack of fit was found (Table 3).

**Step 7:** Payoff matrix and scalarization

The individual constrained maximization of the PCs modeled in step 6 led to the following payoff matrix:

$$\Phi = \begin{bmatrix} 3.216 & -0.402 \\ -0.031 & 1.435 \end{bmatrix} \tag{16}$$

With these values, the scalarization of PC<sub>1</sub> and PC<sub>2</sub> can be done by Eq. (17):

$$\bar{f}(x) = \begin{cases} \overline{PC_1}(x) = \frac{PC_1(x) - 3.216}{-0.402 - 3.216} \\ \overline{PC_2}(x) = \frac{PC_2(x) - 1.435}{-0.031 - 1.435} \end{cases} \tag{17}$$

**Step 8:** NBI method and the Pareto frontier

The minimization of the set of pre-processed responses produced the results presented in Table 6 that were obtained by applying the NBI routine, employing the GRG algorithm available from Microsoft Excel’s Solver®, for the system

of equations as described in Eq. (10). Increments of approximately 5 % were adopted for the weight (*w*) distribution. The nonlinear constraint in this case is  $x^T x \leq 2.829$  since the axial distance  $\rho$  is 1.682.

It can be observed that when higher weights are attributed to the second principal component, the NBI-PCA-SNR approach tends to the MRR optimal values, i.e., higher weights for PC<sub>2</sub> will prioritize productivity in the detriment of quality. The opposite is also true, since when higher weights are attributed to the first principal component, the method tends to the roughness optimal values. This event occurs due to the fact that the first principal component is consist mostly by roughness, while the second principal is consist by MRR.

The Pareto frontier (Fig. 3) for the NBI-PCA-SNR method was built using the data presented in Table 6. The particular form presented by the Pareto frontier can be explained by the convexity of the objective functions. While PC<sub>1</sub> is a convex function, PC<sub>2</sub> is a saddle point. Table 7 shows the eigenvalues of the Hessian matrix of each objective function.

**5 Optimal point by minimization of the global percent error**

Aiming to determine the optimal point of the multiobjective optimization approach discussed in this work, the global optimization by global percent error (GPE) was applied on the set of 21 Pareto-optimal solutions in Table 6. The global percent error indicates the deviation of the Pareto-optimal solutions from the targets defined for the responses and it can be calculated using Eq. (18):

$$GPE = \sum_{i=1}^m \left| \frac{y_i^*}{\zeta_{yi}} - 1 \right| \tag{18}$$

where  $y_i^*$  are the pareto-optimal solutions obtained by the multiobjective optimization and  $\zeta_{yi}$  are the Utopia point (target) for each original response (*R<sub>a</sub>*, *R<sub>t</sub>*, and MRR). The

**Table 8** Global optimization results

Responses	Responses			Cutting parameters		
	<i>R<sub>a</sub></i>	<i>R<sub>t</sub></i>	MRR	<i>V</i>	<i>f</i>	<i>d</i>
Utopia point ( $\zeta_{yi}$ )	1.45	8.75	47.78	220–340	0.08–0.12	0.70–1.20
Optimal point (NBI-SNR-PCA)	1.88	10.75	39.23	286.16	0.13	1.04



optimal point will be the Pareto solution that will give the smaller value for GPE.

The GPE values calculated for each of the 21 Pareto-optimal solutions are presented in Table 6. The smaller value found for GPE was 0.705. The optimal points for the three responses, as well as the optimal levels of the cutting parameters, are presented in Table 8, and they can be compared with the Utopia points ( $\zeta_{yi}$ ) of the original responses.

According to the results presented in Table 8, it can be noted that to maximize the material removal rate while minimizing surface quality, the values that attained the desired quality conditions are the following:  $v=286$  m/min,  $f=0.13$  mm/rev, and  $d=1$  mm. All responses ( $R_a$ ,  $R_t$ , and MRR) optimized by the NBI-PCA-SNR approach were established relatively close to their Utopia point. Therefore, the NBI-PCA-SNR method appears to be very suitable to the optimization of the 12L14 free machining steel turning process.

## 6 Conclusion

This work introduced a mathematical new approach that combine the normal boundary intersection method with principal component analysis and Taguchi's signal-to-noise ratio to optimize a process with multiple correlated responses. Among the several results obtained, the following are worth highlighting:

- The process optimization by the NBI-PCA-SNR method showed a consistent adequacy applied to the 12L14 free machining steel turning process.
- The use of the principal component analysis combined to Taguchi's signal to ratio noise allowed treating the original responses, standardizing the optimization objectives, and eliminating the correlation between the multiple responses.
- For the optimal point found for the NBI-PCA-SNR approach by the minimization of the GPE, cutting speed of 286 m/min, feed rate of 0.13 mm/rev, and depth of cut of 1 mm are the optimal cutting parameters to minimize roughness and maximize removal rate, simultaneously, which should lead to a mean roughness ( $R_a$ ) of 1.88  $\mu\text{m}$ , a total mean roughness ( $R_t$ ) of 10.75  $\mu\text{m}$ , and a removal rate (MRR) of 39.23  $\text{cm}^3/\text{min}$ . These results are shown to be compatible with the bounds for all the responses.
- The results presented in this work confirm that, using technical planning for multiobjective optimization, the turning process can be successfully applied without affecting the machining objectives, in this case, minimum surface roughness and maximum material removal rate.

**Acknowledgments** The authors would like to acknowledge FAPEMIG, Capes, and CNPq for their support of this work.

## Compliance with ethical standards

**Conflict of interest** The authors declare that they have no conflict of interest.

## References

1. Gomes JHF, Júnior ARS, Paiva AP et al (2012) Global criterion method based on principal components to the optimization of manufacturing processes with multiple responses. *J Mech Eng* 58: 345–353. doi:10.5545/sv-jme.2011.136
2. Rao SS (2009) *Engineering optimization: theory and practice*, 4th ed. 829
3. Kulturel-Konak S, Smith AE, Norman BA (2006) Multi-objective tabu search using a multinomial probability mass function. *Eur J Oper Res* 169:918–931. doi:10.1016/j.ejor.2004.08.026
4. Das I, Dennis JE (1998) Normal-boundary intersection: a new method for generating the Pareto surface in nonlinear multicriteria optimization problems. *SIAM J Optim* 8:631–657. doi:10.1137/S1052623496307510
5. Jia Z, Ierapetritou MG (2007) Generate Pareto optimal solutions of scheduling problems using normal boundary intersection technique. *Comput Chem Eng* 31:268–280. doi:10.1016/j.compchemeng.2006.07.001
6. Brito TG, Paiva AP, Ferreira JR et al (2014) A normal boundary intersection approach to multiresponse robust optimization of the surface roughness in end milling process with combined arrays. *Precis Eng* 38:628–638. doi:10.1016/j.precisioneng.2014.02.013
7. Bratchell N (1989) Multivariate response surface modelling by principal components analysis. *J Chemom* 3:579–588. doi:10.1002/cem.1180030406
8. Liao H-C (2006) Multi-response optimization using weighted principal component. *Int J Adv Manuf Technol* 27:720–725. doi:10.1007/s00170-004-2248-7
9. Lim Y, Park Y, Oh H-S (2014) Robust principal component analysis via ES-algorithm. *J Korean Stat Soc* 43:149–159. doi:10.1016/j.jkss.2013.07.002
10. Pontes FJ, Ferreira JR, Silva MB et al (2010) Artificial neural networks for machining processes surface roughness modeling. *Int J Adv Manuf Technol* 49:879–902. doi:10.1007/s00170-009-2456-2
11. Paiva AP, Ferreira JR, Balestrassi PP (2007) A multivariate hybrid approach applied to AISI 52100 hardened steel turning optimization. *J Mater Process Technol* 189:26–35. doi:10.1016/j.jmatprotec.2006.12.047
12. Paiva AP, Campos PH, Ferreira JR et al (2012) A multivariate robust parameter design approach for optimization of AISI 52100 hardened steel turning with wiper mixed ceramic tool. *Int J Refract Met Hard Mater* 30:152–163. doi:10.1016/j.jrmhm.2011.08.001
13. Paiva AP, Costa SC, Paiva EJ et al (2010) Multi-objective optimization of pulsed gas metal arc welding process based on weighted principal component scores. *Int J Adv Manuf Technol* 50:113–125. doi:10.1007/s00170-009-2504-y
14. Lopes LGD, Gomes JHDF, De Paiva AP et al (2013) A multivariate surface roughness modeling and optimization under conditions of

- uncertainty. *Measurement* 46:2555–2568. doi:[10.1016/j.measurement.2013.04.031](https://doi.org/10.1016/j.measurement.2013.04.031)
15. Paiva AP, Paiva EJ, Ferreira JR et al (2009) A multivariate mean square error optimization of AISI 52100 hardened steel turning. *Int J Adv Manuf Technol* 43:631–643. doi:[10.1007/s00170-008-1745-5](https://doi.org/10.1007/s00170-008-1745-5)
  16. Wu F-C (2004) Optimization of correlated multiple quality characteristics using desirability function. *Qual Eng* 17:119–126. doi:[10.1081/QEN-200028725](https://doi.org/10.1081/QEN-200028725)
  17. Zhang M, Anwer N, Stockinger A et al (2013) Discrete shape modeling for skin model representation. *Proc Inst Mech Eng Part B J Eng Manuf* 227:672–680. doi:[10.1177/0954405412466987](https://doi.org/10.1177/0954405412466987)
  18. Johnson RA, Wichern DW (1992) *Applied multivariate statistical analysis*. Pearson Educ 258
  19. Jung JR, Yum BJ (2011) Uniformity and signal-to-noise ratio for static and dynamic parameter designs of deposition processes. *Int J Adv Manuf Technol* 54:619–628. doi:[10.1007/s00170-010-2957-z](https://doi.org/10.1007/s00170-010-2957-z)
  20. Antony J (2001) Simultaneous optimisation of multiple quality characteristics in manufacturing processes using Taguchi's quality loss function. *Int J Adv Manuf Technol* 17:134–138. doi:[10.1007/s001700170201](https://doi.org/10.1007/s001700170201)
  21. Sarıkaya M, Yılmaz V, Dilipak H (2015) Modeling and multi-response optimization of milling characteristics based on Taguchi and gray relational analysis. *Proc Inst Mech Eng Part B J Eng Manuf*. doi:[10.1177/0954405414565136](https://doi.org/10.1177/0954405414565136)